UC Berkeley
UC Berkeley Previously Published Works

Title

Murine Gammaherpesvirus 68 ORF45 Stimulates B2 Retrotransposon and Pre-tRNA Activation in a Manner Dependent on Mitogen-Activated Protein Kinase (MAPK) Signaling

Permalink

Journal

ISSN

Authors

Lari, Azra
Glaunsinger, Britt A

Publication Date

2023-04-13

DOI

Copyright Information

Peer reviewed

Murine Gammaherpesvirus 68 ORF45 Stimulates B2 Retrotransposon and Pre-tRNA Activation in a Manner Dependent on Mitogen-Activated Protein Kinase (MAPK) Signaling

Azra Lari,[a] ![ORCID] Britt A. Glaunsinger[a,b,c]

[a]Department of Plant and Microbial Biology, University of California, Berkeley, Berkeley, California, USA
[b]Department of Molecular and Cell Biology, University of California, Berkeley, Berkeley, California, USA
[c]Howard Hughes Medical Institute, Berkeley, California, USA

ABSTRACT   RNA polymerase III (RNAPIII) transcribes a variety of noncoding RNAs, including tRNA (tRNA) and the B2 family of short interspersed nuclear elements (SINEs). B2 SINEs are noncoding retrotransposons that possess tRNA-like promoters and are normally silenced in healthy somatic tissue. Infection with the murine gammaherpesvirus MHV68 induces transcription of both SINEs and tRNAs, in part through the activity of the viral protein kinase ORF36. Here, we identify the conserved MHV68 tegument protein ORF45 as an additional activator of these RNAPIII loci. MHV68 ORF45 and ORF36 form a complex, resulting in an additive induction RNAPIII and increased ORF45 expression. ORF45-induced RNAPIII transcription is dependent on its activation of the extracellular signal-regulated kinase (ERK) mitogen-activated protein kinase (MAPK) signaling pathway, which in turn increases the abundance of the RNAPIII transcription factor Brf1. Other viral and nonviral activators of MAPK/ERK signaling also increase the levels of Brf1 protein, B2 SINE RNA, and tRNA, suggesting that this is a common strategy to increase RNAPIII activity.

IMPORTANCE   Gammaherpesviral infection alters the gene expression landscape of a host cell, including through the induction of noncoding RNAs transcribed by RNA polymerase III (RNAPIII). Among these are a class of repetitive genes known as retrotransposons, which are normally silenced elements and can copy and spread throughout the genome, and transfer RNAs (tRNAs), which are fundamental components of protein translation machinery. How these loci are activated during infection is not well understood. Here, we identify ORF45 from the model murine gammaherpesvirus MHV68 as a novel activator of RNAPIII transcription. To do so, it engages the MAPK/ERK signaling pathway, which is a central regulator of cellular response to environmental stimuli. Activation of this pathway leads to the upregulation of a key factor required for RNAPIII activity, Brf1. These findings expand our understanding of the regulation and dysregulation of RNAPIII transcription and highlight how viral cooption of key signaling pathways can impact host gene expression.

KEYWORDS   B2, MHV68, RNA polymerase III, SINE, herpesvirus, noncoding RNA, B2 SINE, MAPK, ORF36, ORF45

Mammalian genomes retain a remarkably high number of repetitive sequences derived from transposable elements. Retrotransposons are the largest group among these ancient invasive DNA elements and are defined by the ability to mobilize throughout the genome via RNA intermediates (1, 2). Approximately 10% of the mammalian genome consists of a class of retrotransposons known as short interspersed

nuclear elements (SINEs) (1, 3, 4). SINEs are short (<500 bp), nonautonomous, noncoding retrotransposons transcribed by RNA Polymerase III (RNAPIII). Both human and murine genomes harbor SINE families evolutionarily derived from endogenous RNAPIII transcripts. Alu elements, the predominant family of SINEs in the human genome, and B1 elements in the murine genome are both derived from the 7SL RNA, which is the RNA component of the signal recognition particle (5–7). The unrelated murine B2 SINE family is derived from tRNA (8). Despite their independent origins, human and murine SINEs are ubiquitously present across genomes and are often localized proximal to or within protein-encoding genes (9–11). As such, SINE sequences are known to act as functional enhancers or mobile promoters for proximal genes and can impact the processing, localization, and decay of mRNA transcripts when present as embedded elements (3, 12–27).

Transcription of SINEs is typically repressed in healthy somatic cells in part due to the maintenance of repressive trimethylation of lysine 9 on histone H3 (H3K9) marks and CpG methylation of SINE DNA (28–32). However, in response to cellular stresses, such as chemical treatment, heat stress, or viral infection, SINEs are derepressed and robustly transcribed into SINE noncoding RNAs (ncRNAs) (33–39). Both human and murine SINEs are actively transcribed during infection with several DNA viruses, including herpes simplex virus (HSV-1), adenovirus type 5, minute virus of mice (MVM), simian virus 40 (SV40), and murine gammaherpesvirus 68 (MHV68), which is related to the human gammaherpesviruses Kaposi's sarcoma-associated herpesvirus (KSHV) and Epstein-Barr virus (EBV) (34, 36–40). Upregulation of RNAPIII transcripts during viral infection is not limited to SINEs. Many DNA virus genomes encode their own RNAPIII-transcribed genes whose expression is stimulated by enhanced RNAPIII activity during infection (41–43). Infection with DNA viruses can also enhance transcription and abundance of host premature tRNAs (pre-tRNAs); recent genome-wide studies have identified a global increase in pre-tRNA levels during MHV68 and HSV-1 infection (44, 45).

SINE ncRNAs induced during cellular stress have a variety of documented functions. For example, both Alu and B2 SINE ncRNAs interact directly with RNA Polymerase II (RNAPII) to repress gene expression from individual promoters (46–48). During MHV68 infection, cytoplasmic B2 SINE ncRNAs can activate NF-κB innate immune signaling pathways leading to increased viral replication (39). Constitutive expression of Alu ncRNAs has also been linked to pathogenic outcomes such as age-related macular degeneration (AMD) through activation of the inflammasome, and increased epithelial-to-mesenchymal transition, a hallmark of cancer progression (49–51). Given the array of stresses that induce SINE transcription, there are likely additional functions of SINE ncRNAs yet to be uncovered.

Genome-wide mapping studies in murine fibroblasts identified widespread induction of B2 SINEs and upregulation of ~14% of tRNA loci upon MHV68 infection (44, 52). This induction initiates prior to viral genome replication and is not a consequence of antiviral signaling, nor does it involve Maf1, a central negative regulator of RNAPIII activity (39, 52, 53). A partial screen of MHV68 open reading frames (ORFs) identified a role for the conserved herpesvirus kinase ORF36 in B2 SINE activation, potentially through alterations to the chromatin landscape (53). However, MHV68 mutants lacking functional ORF36 still induce modest levels of SINE RNA, suggesting that additional viral activities contribute to RNAPIII activation.

Here, we identify a second MHV68 protein, ORF45, as an activator of B2 SINE and pre-tRNA transcription during infection. We show that MHV68 ORF45 interacts with ORF36 and together these proteins additively increase RNAPIII transcription. Increased RNAPIII activity requires the ability of ORF45 to stimulate the extracellular signal-regulated kinase (ERK) mitogen-activated protein kinase (MAPK) pathway, which increases the levels of Brf1, an essential component of the RNAPIII transcription factor complex TFIIIB. We show that other activators of MAPK/ERK signaling also enhance Brf1 expression, suggesting that this is a common mechanism to increase RNAPIII activity under conditions where components of the RNAPIII transcriptional machinery are limiting.

RESULTS

MHV68 ORF45 is sufficient to induce B2 SINE transcription and is required for robust B2 SINE and pre-tRNA transcription during MHV68 infection. Previously, we screened a partial library of MHV68 open reading frames (ORFs) and identified ORF36 as an activator of B2 SINE transcription (53). To determine if any additional MHV68 ORFs induce B2 SINE transcription, we cloned and rescreened a portion of the library that included an additional 19 FLAG-tagged ORFs not represented in our prior screen. These were transfected into NIH 3T3 fibroblasts and B2 SINE ncRNA levels were measured by B2 SINE-specific primer extension (Table S1). Among these, the expression of only one additional MHV68 gene was sufficient to upregulate B2 SINEs. Cells expressing FLAG-ORF45, a virion tegument protein conserved among the *Gammaherpesvirinae*, showed a ~2.5-fold increase in B2 SINE ncRNA levels compared to a green fluorescent protein (GFP)-expressing plasmid control (Fig. 1A). In line with prior observations that MHV68 specifically activates B2 SINE and pre-tRNA loci (39, 44), ORF45 did not alter the levels of another RNAPIII-transcribed small nuclear RNA, 7SK. ORF45-mediated induction of B2 SINEs was less pronounced than the ~8-fold induction of B2 SINEs by ORF36, perhaps due to the lower expression levels of FLAG-ORF45 compared to FLAG-ORF36 (Fig. 1B). Nonetheless, B2 SINE transcriptional activation was consistently specific to only ORF45 or ORF36 and not observed with other MHV68 ORFs such as ORF65 (Fig. 1A, Table S1).

We next sought to assess the contribution of ORF45 toward B2 SINE and pre-tRNA transcriptional activation during infection. ORF45 is an essential MHV68 gene, and we were unable to delete it in the virus, so to deplete it from infected cells we instead generated 3T3 fibroblast cell lines constitutively expressing control or ORF45-targeting shRNAs (54). The ORF45-targeting shRNAs partially reduced ORF45 protein expression 24 h postinfection (hpi) with MHV68 compared to the control shRNA cell line, whereas expression of the ORF65 capsid protein was largely unaffected (Fig. 1C). Reduced ORF45 levels scaled with a reduction in MHV68-induced B2 RNA as measured by primer extension, and in pre-tRNA induction as measured by quantitative reverse transcriptase PCR (RT-qPCR) using primer sets that were specific for the pre-tRNAs produced from the intron-containing tRNA-TYR gene (Fig. 1D and E). From these data, we conclude that ORF45 contributes to RNAPIII transcriptional activation during MHV68 infection.

MHV68 ORF45 and ORF36 interact and additively upregulate B2 SINE and pre-tRNA transcription. In KSHV, the ORF45 and ORF36 proteins interact (55), which is notable given that these are the two MHV68 ORFs involved in RNAPIII activation. In streptavidin-based affinity purification experiments, we similarly found that N-terminally Strep-tagged MHV68 ORF45 interacted with N-terminally FLAG-tagged MHV68 ORF36 (Fig. 2A). Also, in line with studies of the KSHV protein homologs (55), expression of MHV68 ORF36 resulted in increased levels of the ORF45 protein (Fig. 2B). This did not appear to be a mutually stabilizing interaction, as ORF36 protein levels were unaffected by cotransfection of ORF45 (Fig. 2B).

Given that both ORF45 and ORF36 can independently activate RNAPIII transcription and that their interaction boosts ORF45 expression, we considered whether their interaction additively or synergistically impacted RNAPIII transcriptional activation. Cells coexpressing Strep-ORF45 and FLAG-ORF36 displayed an additive increase of B2 SINE ncRNA expression (~7-fold) compared to cells only expressing ORF45 (~3-fold) or ORF36 (~5-fold) (Fig. 2C). Similarly, pre-tRNA^{TYR} levels increased by ~3 and ~9-fold in the presence of ORF45 or ORF36, respectively, and additively increased to ~15-fold upon their cotransfection (Fig. 2D). Thus, although MHV68 ORFs 45 and 36 interact, their stimulation of RNAPIII transcription may occur by distinct mechanisms.

The ORF45 NLS and conserved C-terminal domain are dispensable for B2 SINE induction. Both KSHV ORF45 and MHV68 ORF45 contain nuclear localization signals and can traffic between the nucleus and the cytoplasm; however, KSHV ORF45 is predominantly localized to the cytoplasm while MHV68 ORF45 is predominantly localized to the nucleus (54, 56). Deletion of the MHV68 ORF45 nuclear localization signal (Strep-ORF45-ΔNLS) shifted its localization largely to the cytoplasm as measured by immunofluorescence assay (Fig. 3A). Despite this shift in localization, Strep-ORF45-ΔNLS
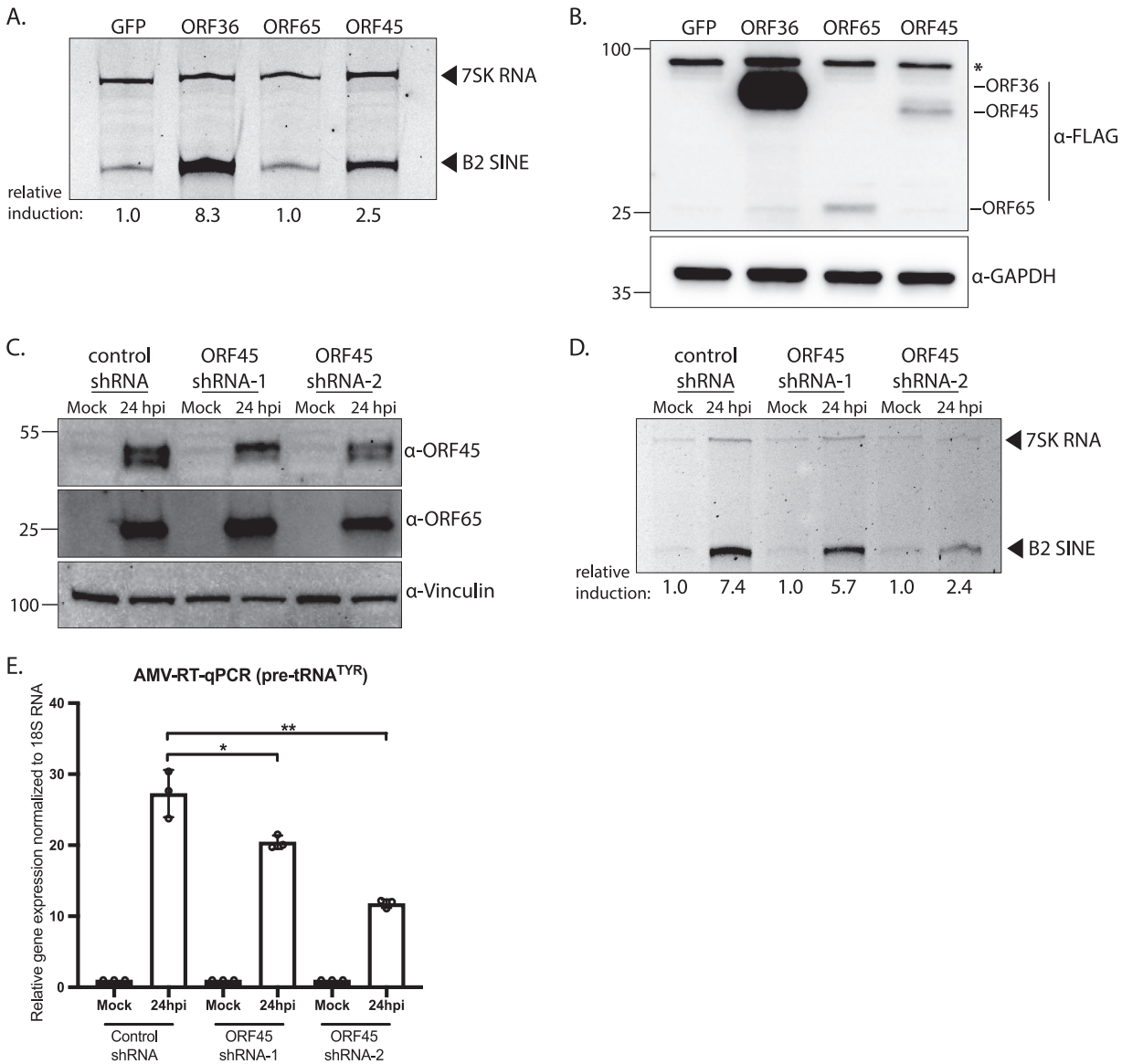
FIG 1 MHV68 ORF45 contributes to B2 SINE and pre-tRNA transcription during MHV68 lytic infection. (A) NIH 3T3 cells were transfected with plasmids containing the indicated N-terminally FLAG-tagged MHV68 ORFs or GFP-expressing control for 24 h, whereupon total RNA was subjected to primer extension using primers specific to B2 SINE ncRNAs or 7SK RNA (control). In this and all subsequent primer extensions, the relative induction of B2 SINE ncRNAs for each sample was measured as the ratio of the mean integrated intensity between 7SK RNA and B2 SINE ncRNA levels and normalized to the control (GFP-expressing plasmid) ratio. (B) Protein extracted from cells harvested from panel A was analyzed by Western blotting with antibodies against FLAG and GAPDH (loading control). The asterisk (*) represents a nonspecific band. (C) Stable NIH 3T3 cell lines constitutively expressing a control shRNA or ORF45-targeting shRNAs (shRNA-1 or shRNA-2) were mock-infected or infected with MHV68 at an MOI of 5. At 24 hpi, cells were harvested and lysed to extract total protein and were analyzed by Western blotting with antibodies against MHV68 ORF45, ORF65, and Vinculin (loading control). (D) Cells from panel C were also harvested for total RNA extraction and subjected to primer extension using primers specific to B2 SINE ncRNAs or 7SK RNA (control). (E) Total RNA extracted from panel D was also used to detect pre-tRNA^{TYR} levels with forward and reverse primers with 3' ends complementary to the tRNA intron using AMV RT-qPCR. Expression was normalized to 18S rRNA and compared to values from mock-infected cells. RT-qPCR experiments were done in triplicate. Error bars show the standard deviation (SD), and statistics were calculated using an unpaired t test on raw ΔC_T values. ns, not significant; *, $P < 0.05$; **, $P < 0.01$.

activated B2 SINE transcription to comparable levels as WT ORF45, suggesting that a predominantly nuclear localization may be dispensable for B2 SINE activation (Fig. 3B).

Gammaherpesvirus ORF45 homologs share very low amino acid sequence identity, although the C-terminal region is the most conserved and is required for transcomplementation of an MHV68 ORF45-null mutant virus (54). The last 23 amino acids of the MHV68 ORF45 C terminus share 58% similarity to the C terminus of KSHV ORF45, 50% to the EBV homolog BKRF4, and 39% to the Rhesus rhadinovirus (RRV) ORF45 homolog
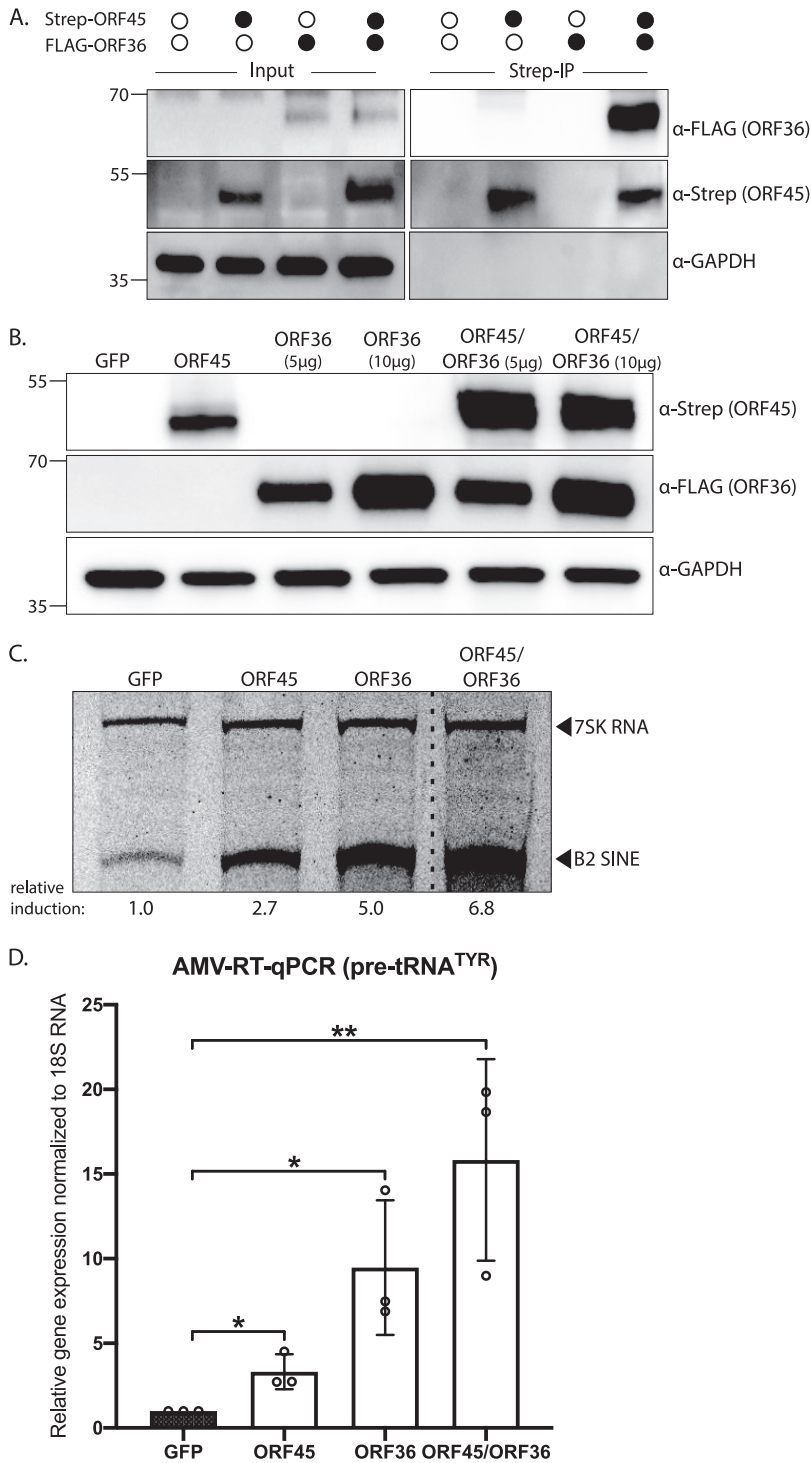
FIG 2 MHV68 ORF45 and ORF36 interact and mutually enhance B2 SINE and pre-tRNA transcription. (A) NIH 3T3 fibroblasts were transfected with Strep-ORF45 and/or FLAG-ORF36 and lysates were purified over StrepTactin XT magnetic beads followed by Western blotting with antibodies against Strep, FLAG, and GAPDH (loading control). (B) NIH 3T3 fibroblasts were transfected with Strep-ORF45, FLAG-ORF36, or a GFP control for 24 h. Protein lysates were analyzed by Western blotting with antibodies against Strep, FLAG, and GAPDH (loading control). (C and D) RNA extracted from cells harvested in panel B was subjected to either primer extension using primers specific to B2 SINE ncRNAs or 7SK RNA (as a control) (C), or RT-qPCR to detect pre-tRNA^{TYR} (D). The dashed line indicates where an irrelevant lane was removed from the image (C). Pre-tRNA^{TYR} levels were normalized to 18S rRNA and compared to values from the GFP-expressing control (D). RT-qPCR experiments were done in triplicate. Error bars show the standard deviation (SD), and statistics were calculated using an unpaired t test on raw ΔC_T values. ns, not significant; *, $P < 0.05$; **, $P < 0.01$.
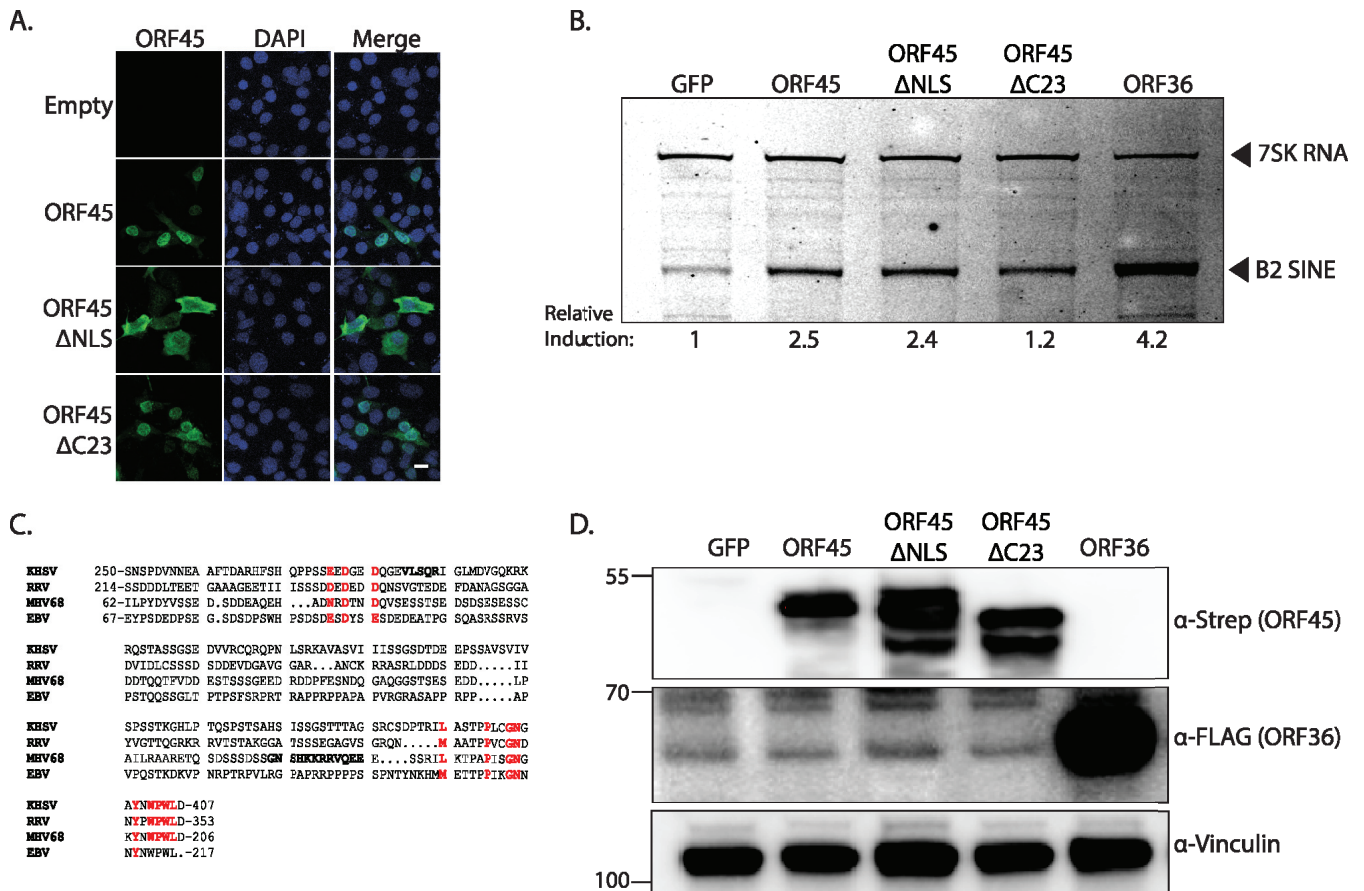
FIG 3 The ORF45 NLS and C-terminal residues are dispensable for B2 SINE transcriptional activation. (A) Confocal microscopy images of NIH 3T3 cells transfected with an empty control vector or the indicated Strep-tagged ORF45 plasmids and incubated with anti-Strep antibodies to detect ORF45 (green) or DAPI to identify nuclei (blue), with the right panels showing merged images. Scale bar = 5 μm. (B) NIH 3T3 cells were transfected with plasmids containing indicated Strep-tagged genes or a GFP control for 24 h, whereupon cells were harvested for total RNA extraction and subjected to primer extension using primers specific to B2 SINE ncRNAs or 7SK RNA (control). (C) Sequence alignment of ORF45 homologs. The diagram shows the most conserved regions of KSHV ORF45 (amino acids 250 to 407), EBV BKRF4 (amino acids 67 to 217), MHV68 ORF45 (amino acids 62 to 206), and RRV ORF45 (amino acids 214 to 253). NLS sequences in KSHV and MHV68 ORF45 are bolded, and residues showing the highest consensus across the sequences are highlighted in red (D) Protein lysates from cells harvested from panel B were analyzed by Western blotting with antibodies against Strep, FLAG, and Vinculin (loading control).

(Fig. 3C) (54). However, deletion of the C-terminal 23 amino acids (ORF45-ΔC23) resulted in only a modest reduction of B2 SINE transcriptional activation (Fig. 3B). WT ORF45 exhibited the characteristic protein doublet indicative of phosphorylation, but the banding pattern of the mutants was different, suggesting that these residues may directly or indirectly influence the modification state of ORF45 (Fig. 3D). Although it remains unclear which phosphorylated form of ORF45 contributes to B2 SINE transcriptional upregulation, these data demonstrate that neither strong nuclear localization nor the conserved C-terminal region of MHV68 ORF45 is essential for RNAPIII activation.

Upregulation of RNAPIII activity by MHV68 ORF45 requires stimulation of MAPK/ERK signaling. KSHV ORF45 interacts with the cellular p90 ribosomal S6 kinase (RSK1/2) and forms a ternary complex with the extracellular signal-regulated kinase (ERK2) of the mitogen-activated protein kinase (MAPK) pathway, strongly stimulating their kinase activities (57–63). This correlates with sustained phosphorylation of RSK1/2 and ERK1/2, which are functional mediators of MAPK/ERK signaling, and are important for MHV68 lytic infection (64). We first examined whether the kinetics of ORF45 protein expression matched the accumulation of phosphorylated (i.e., active) ERK1/2 during MHV68 lytic infection. Indeed, there was a correlation between ORF45 expression, which initiates at 8 hpi and increases dramatically at 16 to 24 hpi (54), and the

abundance of phosphorylated ERK1/2 (Fig. 4A). Accumulation of B2 SINE RNAs and pre-tRNA^{TYR} also matched these kinetics (Fig. 4B and C). Together, these data demonstrate that ORF45 expression, MAPK/ERK activation, and RNAPIII transcript induction are temporally coincident.

In agreement with data for KSHV ORF45, transfection of MHV68 Strep-ORF45 greatly increased the abundance of phosphorylated ERK1/2, indicative of activated MAPK/ERK signaling (Fig. 4D). Amino acids 29 to 146 of MHV68 ORF45 are most similar to the previously identified RSK/ERK activation domain of KSHV ORF45 (65). Expression of an ORF45 deletion mutant lacking a portion of this region (Strep-ORF45-Δ46-106) resulted in reduced levels of phosphorylated ERK1/2; however, this large deletion also impaired ORF45 protein expression, confounding the interpretation of its activity (Fig. 4D). We tested additional mutants and ultimately determined that a smaller deletion of amino acids 61 to 75 (ORF45-Δ61-75) resulted in protein expression levels comparable to the full-length protein yet did not activate ERK1/2 (Fig. 4E, Fig. S1). Unlike full-length ORF45 or the ORF36 control, ORF45-Δ61-75 failed to induce B2 SINE RNA as measured by primer extension (Fig. 4F).

To determine if the ORF45-mediated activation of ERK1/2 contributed to the transcriptional upregulation of B2 SINEs and pre-tRNAs observed during MHV68 lytic infection, we used a highly selective inhibitor (U0126) of the ERK kinases Mek1/2 (66). Intriguingly, while U0126 treatment reduced the levels of phosphorylated ERK1/2 during infection, it also significantly reduced ORF45 protein levels (Fig. 4G). This suggests that activation of ERK by ORF45 creates a positive feedback loop that boosts ORF45 expression. Notably, the reduction in phosphorylated ERK and ORF45 led to a decrease in B2 SINE and pre-tRNA transcriptional activation during infection relative to the dimethyl sulfoxide (DMSO)-treated controls (Fig. 4H and I). Overall, these data validate a role for MHV68 ORF45 in the activation of cellular MAPK/ERK signaling, identify an ERK activation domain within MHV68 ORF45, and demonstrate a connection between ORF45-mediated MAPK/ERK signaling and RNAPIII transcriptional activation during infection.

Constitutive activation of MAPK/ERK signaling leads to B2 SINE and pre-tRNA upregulation through increased levels of Brf1. Several connections exist between RNAPIII activity and mitogenic factors such as ERK. Most notably, ERK directly binds and activates components of the essential RNAPIII transcription factor complex, TFIIIB, and the levels of the essential TFIIIB component Brf1 increase in response to cellular growth stimuli in specific cell types (67–70). We previously showed that depletion of Brf1 completely abrogates the expression of B2 SINEs during MHV68 infection (53). Therefore, one possible mechanism whereby ORF45 might increase RNAPIII activity is by boosting the levels of Brf1. Indeed, while endogenous Brf1 protein was barely detectable in NIH 3T3 fibroblasts transfected with a control GFP plasmid, its levels markedly increased upon transfection of ORF45 (Fig. 5A). This was dependent on the activation of ERK signaling, as Brf1 levels did not increase in cells containing the ORF45-Δ61-75 mutant (Fig. 5A). It was also notable that MHV68 ORF36 did not alter Brf1 levels, indicating that its RNAPIII induction occurs via a mechanism distinct from that of ORF45 (Fig. 5A).

Finally, to determine whether ERK activation was sufficient to upregulate Brf1 and induce transcription of B2 SINEs and pre-tRNA, we activated ERK signaling through two ORF45-independent mechanisms. We expressed either a constitutively active form of the small GTPase H-Ras (Ras-V12) (71), or the HSV-1 ICP0 protein, which is a predicted stimulator of MAPK/ERK signaling during infection (72). Indeed, compared to the GFP control plasmid, both Ras-V12 and HSV-1 ICP0 transfection resulted in an increase in Brf1 protein levels (Fig. 5B), as well as enhanced expression of B2 SINE ncRNAs and pre-tRNA^{TYR} levels (Fig. 5C and D). These levels were comparable to the levels of transcriptional enhancement induced by ORF45 (Fig. 2C and D).

Collectively, these data support a model whereby the ERK activation function of ORF45 increases RNAPIII transcription by elevating the levels of Brf1 in cells where its expression is limiting. This mechanism likely extends to other viral activators of MAPK/ERK signaling that regulate RNAPIII activity during viral infection.
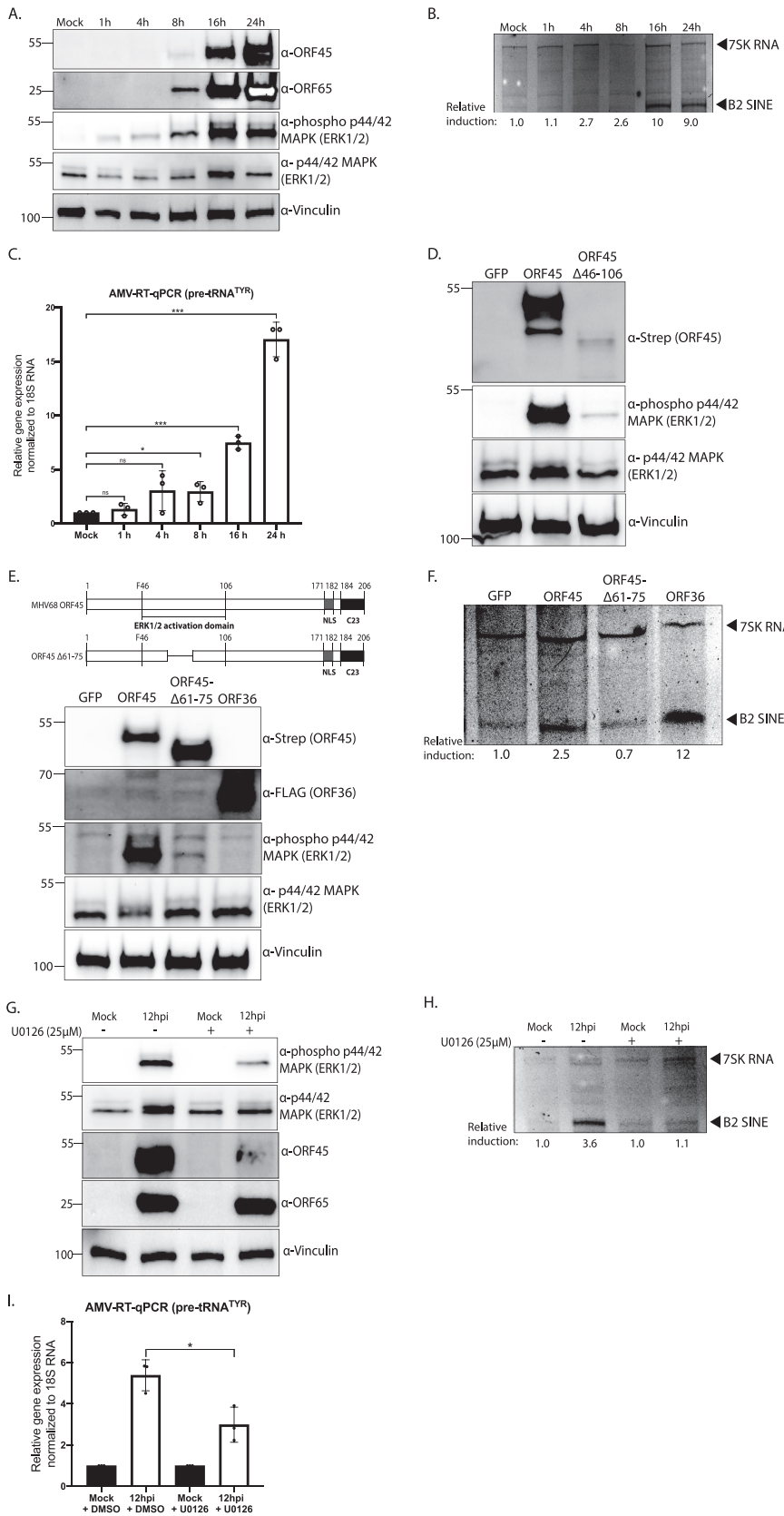
FIG 4 MHV68 ORF45-induced MAPK/ERK signaling is required for B2 SINE and pre-tRNA induction. (A) NIH 3T3 fibroblasts were mock-infected or infected with MHV68 at an MOI of 5 for 1, 4, 8, 16, or 24 h. At the indicated time point, cells were harvested and lysed to extract total protein and were

DISCUSSION

RNAPIII transcription is modulated during infection with several DNA viruses, leading to the upregulation of specific cellular RNAPIII transcripts (34, 37–40, 44, 45, 73–75). Together with our prior work (53), we have now screened 90% of the known MHV68 ORFs (76) and identified two, ORF36 and ORF45, as having independent RNAPIII activation functions. Both MHV68 ORF36 and ORF45 are required for efficient viral replication and viral gene expression, and ORF45 is also involved in virion morphogenesis (54, 77, 78). ORF36 and ORF45 are early and early-late genes, respectively (79, 80), consistent with the viral DNA replication-independent early and late kinetics of B2 SINE and pre-tRNA transcriptional activation (39, 44). Although the mechanistic details of how ORF36 activates RNAPIII transcription remain unknown, it is proposed to function by inhibiting proteins involved in the maintenance of a repressive chromatin landscape (53). Our mutational analysis of MHV68 ORF45 revealed that its stimulation of RNAPIII transcription is coordinated in the cytoplasm through its ability to activate MAPK/ERK signaling. Cytoplasmic ORF45 may propagate a signaling cascade that enhances Brf1 transcription in the nucleus, or perhaps ORF45-phosphorylated ERK increases the protein stability of Brf1 in the cytoplasm. Notably, while the impact of ORF36 and ORF45 on RNAPIII activation is additive and thus likely to occur via distinct mechanisms, these proteins physically interact, underscoring their potential coordination during infection. Altogether, these data provide novel insight into the function of ORF45 and link cellular MAPK signaling to RNAPIII transcriptional activity in the context of viral infection.

Our data suggest that MHV68 ORF45 displays functional conservation with KSHV ORF45, despite sharing little sequence identity. Like their KSHV homologs, we show here that MHV68 ORF45 and ORF36 stably interact (55). In KSHV, ORF36 is a substrate of ORF45-activated kinases and ORF45 enhances the kinase activity of ORF36; although untested, this may similarly occur for the MHV68 homologs. KSHV ORF45 causes sustained activation of p90 ribosomal kinases (RSKs) and extracellular regulated kinases (ERKs) (57–62), and subsequent studies also identified that KSHV ORF45, ORF36, and RSK form a stable complex (55, 63). Another function of KSHV ORF45 is suppression of interferon regulatory factor 7 (IRF7), a crucial regulator of type I interferon gene expression (81–83). Given that both IRF3 and IRF7 are dispensable for B2 SINE transcriptional activation during MHV68 infection (53), if MHV68 ORF45 retains this function, we hypothesize it would not be linked to RNAPIII activity.

FIG 4 Legend (Continued)

analyzed by Western blotting with antibodies against MHV68 ORF45, ORF65, phospho-ERK1/2, ERK1/2, and Vinculin (loading control). (B) Cells from panel A were also harvested for total RNA extraction and subjected to primer extension using primers specific to B2 SINE ncRNAs or 7SK RNA (control). (C) Total RNA extracted from panel A was also used to detect pre-tRNA^{TYR} levels with forward and reverse primers with 3′ ends complementary to the tRNA intron using AMV RT-qPCR. Expression was normalized to 18S rRNA and compared to values from mock-infected cells. RT-qPCR experiments were done in triplicate. Error bars show the standard deviation (SD), and statistics were calculated using an unpaired t test on on raw ΔC_T values. ns, not significant; *, $P < 0.05$; **, $P < 0.01$; ***, $P < 0.001$. (D) NIH 3T3 fibroblasts were transfected with indicated Strep-tagged genes or a GFP control for 24 h, whereupon lysates were analyzed by Western blotting with antibodies against Strep, phospho-ERK1/2, ERK, and Vinculin (loading control). (E) NIH 3T3 fibroblasts were transfected with Strep-tagged ORF45, ORF45Δ61-75, FLAG-tagged ORF36, or a GFP control for 24 h, whereupon lysates were analyzed by Western blotting with antibodies against Strep, FLAG, phospho-ERK1/2, ERK, and Vinculin (loading control). (F) Cells from panel E were also harvested for total RNA extraction and subjected to primer extension using primers specific to B2 SINE ncRNAs or 7SK RNA (control). (G) NIH 3T3 fibroblasts were mock-infected or infected with MHV68 at an MOI of 5 and treated with DMSO (control) or U0126 (25 μM) for 12 h. Cells were harvested and lysed to extract total protein and were analyzed by Western blotting with antibodies against MHV68 ORF45, ORF65, phospho-ERK1/2, ERK1/2, and Vinculin (loading control). (H) Cells from panel G were also harvested for total RNA extraction and subjected to primer extension using primers specific to B2 SINE ncRNAs or 7SK RNA (control). (I) Total RNA extracted from panel G was also used to detect pre-tRNA^{TYR} levels with forward and reverse primers with 3′ ends complementary to the tRNA intron using AMV RT-qPCR. Expression was normalized to 18S rRNA and compared to values from mock-infected cells. RT-qPCR experiments were done in triplicate. Error bars show the standard deviation (SD), and statistics were calculated using an unpaired t test on raw ΔC_T values. ns, not significant; *, $P < 0.05$.
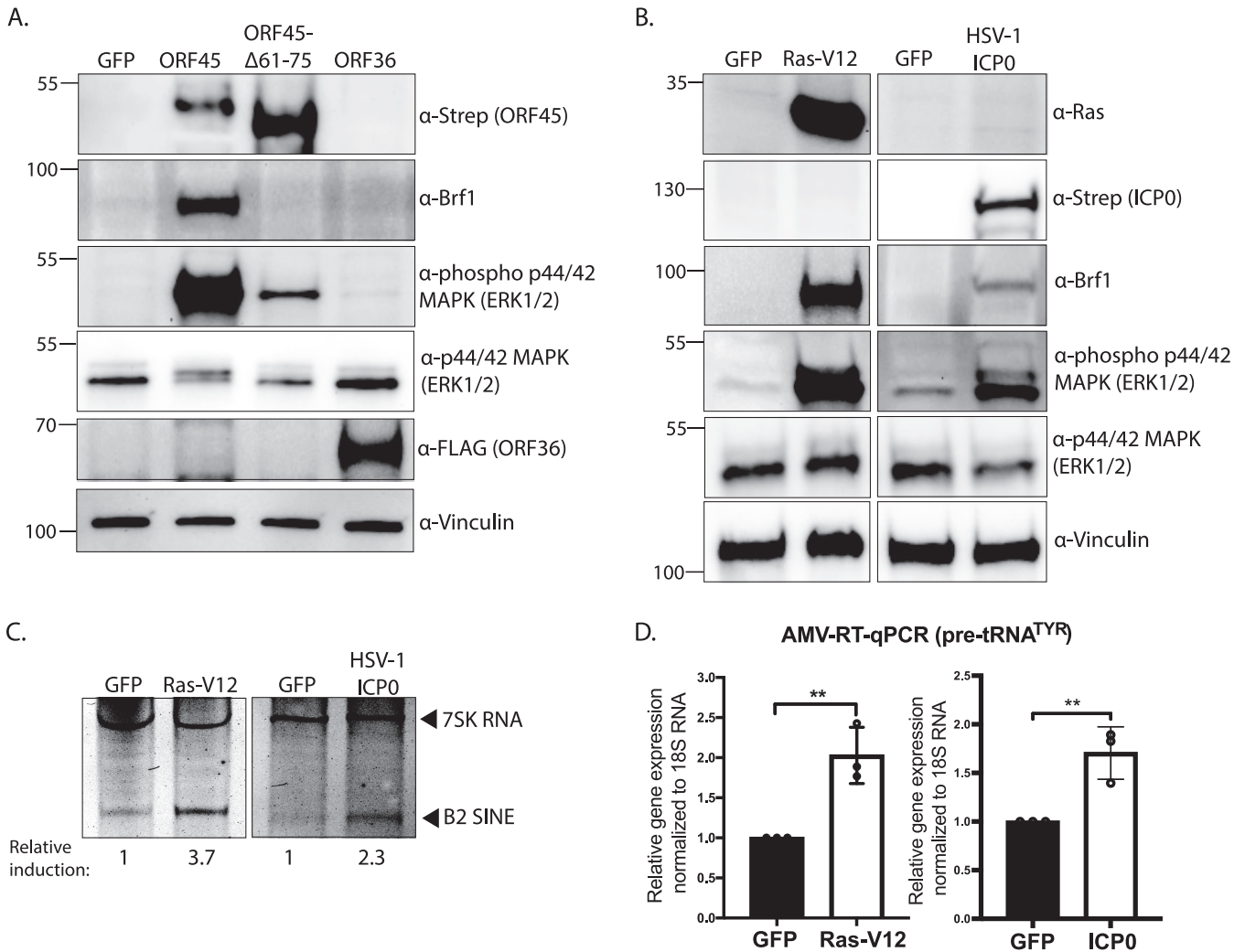
FIG 5 Constitutive activation of MAPK/ERK signaling upregulates Brf1 and enhances RNAPIII transcription. NIH 3T3 fibroblasts were transfected with the indicated expression plasmids for 24 h. (A and B) Protein lysates were analyzed by Western blotting with the indicated antibodies. Vinculin served as a loading control. (C and D) Total RNA was also extracted from the samples in panel B and subjected to primer extension using primers specific to B2 SINE ncRNAs or 7SK RNA (as a control) (C) or RT-qPCR to detect pre-tRNA^{TYR} levels, whose expression was normalized to 18S rRNA and compared to values from the GFP-expressing control (D). RT-qPCR experiments were done in triplicate. Error bars show the standard deviation (SD), and statistics were calculated using an unpaired t test on raw ΔC_T values. ns, not significant; *, $P < 0.05$; **, $P < 0.01$.

Studies in proliferating mammalian cells have been critical in understanding the connection between cellular regulators of proliferation (e.g., ERK1/2) and RNAPIII transcriptional regulation. Upon mitogenic stimulation, cell growth is accompanied by ERK activation and a rapid increase in RNAPIII transcription (84–86). Activated ERK2 induces RNAPIII transcription through phosphorylation of Brf1, an essential component of the RNAPIII transcription factor TFIIIB (69). Phosphorylation of Brf1 enhances promoter recruitment of TFIIIB and RNAPIII, increasing the transcriptional output of RNAPIII. Brf1 can be limiting for the type 2 RNAPIII promoters found in tRNAs and B2 SINEs, with several cell types exhibiting low basal levels of Brf1 (67, 69, 87, 88). Indeed, we observed very low basal Brf1 levels in murine fibroblasts and found that ORF45-induced ERK activation led to an increase in Brf1 protein expression. We hypothesize that this may be a viral strategy to overcome limiting levels of Brf1, thereby facilitating RNAPIII activation in MHV68-infected cells.

Many DNA and RNA viruses hijack the MAPK/ERK signaling cascade to mediate viral internalization, dysregulate the cell cycle, regulate viral replication, and prevent cell death (89–92). MAPK/ERK signaling promotes viral reactivation from latency during KSHV infection, viral replication during lytic MHV68 infection, and the production of

TABLE 1 Primers used in this study

Primer	Name	Sequence (5′–3′)	Purpose
1	3xFLAG-ORF45-F	gacaaggggggcggccgacccctttaagaaaccagtgaga	Cloning
2	3xFLAG-ORF45-R	gccctctagactcgatcaatccaaccatggccagt	Cloning
3	3xFLAG-ORF65-F	gacaaggggggcggccaataaagacagggtcaaagctcc	Cloning
4	3xFLAG-ORF65-R	gccctctagactcgactactttttctttccatttccactc	Cloning
5	2xStrep-ORF45-F	gagaaggggggcggccgacccctttaag	Cloning
6	2xStrep-ORF45-R	gccctctagactcgagtcaatccaaccatggc	Cloning
7	ORF45-ΔNLS-F	cagttccgaaagtagtcgcatcttg	Mutagenesis
8	ORF45-ΔNLS-R	ctactttcggaactgtcactagagc	Mutagenesis
9	ORF45-ΔC23-F	gaaagttgactcgagtctagaggg	Mutagenesis
10	ORF45-ΔC23-F	ctcgagtcaactttcttcttcctgc	Mutagenesis
11	ORF45-Δ46-106-F	tgtgacgatacccagcagactttc	Mutagenesis
12	ORF45-Δ46-106-R	cactgagtctggagttgatgaccc	Mutagenesis
13	ORF45-Δ61-75-F	gaagcacaagaacatgcggtaaac	Mutagenesis
14	ORF45-Δ61-75-R	ggcgggagttggaggagttcttg	Mutagenesis
15	2xStrep-ICP0-F1	gagaaggggggcggccgagcctcgaccc	Cloning
16	2xStrep-ICP0-R2	tctgcctcgaccacaccaac	Cloning
17	2xStrep-ICP0-F2	tgtggtcgaggcagaagcg	Cloning
18	2xStrep-ICP0-F2	gccctctagactcgactactgtttgcc	Cloning
19	shRNA-ORF45-1-F	ccgggtgcaggaagaagaaagtagtctcgagactactttcttcttcctgcacttttttg	shRNA oligonucleotide
20	shRNA-ORF45-1-R	aattcaaaaagtgcaggaagaagaaagtagtctcgagactactttcttcttcctgcac	shRNA oligonucleotide
21	shRNA-ORF45-2-F	ccggcagtgagaatgttgcccataactcgagttatgggcaacattctcactgttttttg	shRNA oligonucleotide
22	shRNA-ORF45-2-R	aattcaaaaacagtgagaatgttgcccataactcgagttatgggcaacattctcactg	shRNA oligonucleotide
23	pre-tRNA^{TYR}-F	ccttcgatagctcagttggtagagc	qPCR
24	pre-tRNA^{TYR}-R	ggattcgaaccagcgacctaaggatatc	qPCR
25	18S RNA-F	gtaacccgttgaacccatt	qPCR
26	18S RNA-R	ccatccaatcggtagtagcg	qPCR
27	FAM-B2 SINE	/56-FAM/tacactgtagctgtcttcagaca	Primer extension
28	FAM-7SK	/56-FAM/tgagcttgtttggaggttct	Primer extension

infectious progeny during both MHV68 and KSHV infection (64, 93–101). The pro-viral nature of MAPK/ERK activation is consistent with findings that B2 SINE ncRNAs enhance viral gene replication and expression (39). Although ORF45 is only conserved among gammaherpesviruses, the alphaherpesvirus HSV-1 strongly induces RNAPIII transcription of endogenous human SINE elements (Alus) (37). Here, we show one example of an HSV-1 viral protein (ICP0) that has been previously linked to ERK activity during infection (72), activates ERK signaling, increases Brf1 protein levels, and enhances B2 SINE and pre-tRNA transcription upon transfection in murine fibroblasts. Interestingly ICP4, which has been identified to play a role in RNAPIII activation during HSV-1 infection, functionally interacts with ICP0 (37, 102). It is possible that there are additional viral activators of MAPK/ERK signaling, whose characterization should yield new insights into the regulation of noncoding RNA production during infection.

MATERIALS AND METHODS

Plasmids and cloning. MHV68 FLAG-tagged ORF45 and ORF65 were subcloned into the XhoI and NotI sites of pcDNA4/TO-3xFLAG (N-terminal tag) to generate pcDNA4/TO-3xFLAG-ORF45 or ORF65 using InFusion cloning (Clontech). ORF45 and ICP0 were subcloned into the BamHI and XhoI sites of pcDNA4/TO-2xStrep (N-terminal tag) to generate pcDNA4/TO-2xStrep-ORF45 using InFusion cloning. Deletion mutants of 2xStrep-ORF45 were generated using site-directed mutagenesis PCR with Q5 DNA polymerase (New England Biolabs) with primers listed in Table 1. PCR products were DpnI treated, ligated using T4 polynucleotide kinase and T4 DNA ligase, and transformed into *Escherichia coli* XL-1 Blue cells. To generate pLKO.1-ORF45 shRNA-1 and pLKO.1-ORF45 shRNA-2 for lentivirus transductions, the pLKO.1 TRC cloning vector (Addgene plasmid 10879) was digested with EcoRI and AgeI to release a 1.9-kb stuffer. shRNA oligonucleotides targeting ORF45 listed in Table 1 were then annealed and ligated into the vector using T4 DNA ligase (New England Biolabs) and transformed into *Escherichia coli* XL-1 Blue cells. The packaging plasmids pMD2.G (Addgene plasmid 12259) and psPAX2 (Addgene plasmid 12260) were also used to generate lentivirus. All newly generated plasmids have been deposited to Addgene https://www.addgene.org/Britt_Glaunsinger/.

Cell lines and transductions. NIH 3T3 (ATCC CRL-1658) and NIH 3T12 (ATCC CCL-164) mouse fibroblast cell lines and HEK293T human cell lines (ATCC CRL-3216) were maintained in Dulbecco's modified Eagle's medium (DMEM; Gibco) with 10% fetal calf serum (FBS; VWR) and screened regularly for

mycoplasma by PCR. To generate transduced NIH 3T3 cell lines stably expressing a control shRNA or MHV68 ORF45 targeting shRNAs, lentivirus was generated in HEK293T cells by cotransfection of the pLKO.1 TRC cloning control vector or ORF45 expression shRNA vectors along with packaging plasmids. Twenty-four hours after transfection, the medium was replaced with fresh DMEM supplemented with 10% FBS and 10 μg/mL bovine serum albumin (BSA; Invitrogen). After 48 h, the supernatant was harvested, and syringe filtered through a 0.45-μm pore size filter (Millipore). Polybrene was added to a final concentration of 8 μg/mL to freshly trypsinized NIH 3T3 cells (3×10^6) and cells were spinoculated with 2 mL of the lentivirus containing supernatant in a 12-well plate for 2 h at $1,000 \times g$. After 24 h, the cells were expanded to a 10-cm tissue culture plate and selected for 1 week in media supplemented with 2 μg/mL puromycin (MilliporeSigma).

Transfections. Transfections of MHV68 ORF containing plasmids into NIH 3T3 fibroblasts were completed as follows: 3T3 cells were maintained in DMEM with 10% FBS and grown to 90% confluence. Cells were removed and washed once with Dulbecco's phosphate-buffered saline (DPBS) (Gibco). Transfections were done using the Neon Transfection System (Thermo Fisher). Then, 2×10^6 cells were resuspended in 100 μL of buffer R, to which GFP (30 μg), ORF45 (30 μg), ORF65 (30 μg), ORF36 (5 or 10 μg), ICP0 (30 μg), or Ras-V12 (20 μg) plasmid DNA was added (in the cases where less than 30 μg of DNA was used, empty pcDNA4/TO-vector was added to equal 30 μg of total plasmid DNA). This was loaded into a Neon 100-μL pipette tip and Neon tube with 3 mL of buffer E2 with electroporation parameters set to 1,300 V, 20 ms, 2 pulses. Following electroporation, cells were plated in 2 mL of DMEM with 10% FBS in 6-well TC-treated plates and were incubated at 37°C for 24 h.

Virus preparations and infections. MHV68 was amplified in NIH 3T12 fibroblast cells, and the viral 50% tissue culture infective dose (TCID50) was measured on NIH 3T3 fibroblasts by limiting dilution. NIH 3T3 fibroblasts were infected at the indicated multiplicity of infection (MOI) by adding the required volume of the virus to cells in 5 mL of serum-free DMEM in 10-cm TC-treated plates. Infection was allowed to proceed for 1 h to allow for viral entry followed by removal of the virus-containing media and replacement with fresh DMEM with 10% FBS. Cells were harvested at the indicated time points postinfection and were treated with 25 μM of U0126 (Cell Signaling) or DMSO, as indicated.

Primer extension and RT-qPCR. Total RNA was extracted from cells using TRIzol reagent (Invitrogen). Primer extension was performed on 15 μg of total RNA using a 5′-fluorescein-labeled oligonucleotides specific to B2 SINE RNA or 7SK RNA. RNA was ethanol precipitated in 1 mL 100% EtOH, washed in 70% ethanol, and pelleted at $21,130 \times g$ and 4°C for 10 min. Pellets were resuspended in 18 μL of 1X SuperScript III reverse transcriptase reaction buffer (SSIII-RT; Thermo Fisher) containing 1 μL of each 5′-fluorescein-labeled primer (10 pmol/μL) listed in Table 1. Samples were heated to 80°C for 10 min, followed by annealing for 1 h at 56°C. Then, 30 μL of extension buffer (1X SSIII-RT buffer, 40U RNasin RNase Inhibitor [Promega] 2 mM DTT, 1 mM dNTP, 1,000 U of SSIII-RT) was added, and extension was carried out for 1 h at 42°C. Samples were precipitated in 100% ethanol for 20 min at −80°C, and then pellets were briefly air dried and resuspended in 20 μL 1× RNA loading dye (47.5% formamide, 0.01% SDS, 0.01% bromophenol blue, 0.005% xylene cyanol, and 0.5 mM EDTA). Then, each sample was run on an 8% urea-PAGE gel for 1 h at 250 V. Gels were imaged on a Chemidoc imager (Bio-Rad) with fluorescein imaging capability. Relative induction of B2 SINE ncRNAs for each sample was measured as the ratio of the mean integrated intensity between 7SK RNA and B2 SINE ncRNA level using FIJI (103) and was normalized to the GFP-expressing plasmid control. For RT-qPCR, total RNA was isolated from cells using TRIzol (Invitrogen), treated with Turbo DNase (Ambion), and reverse transcribed with AMV RT (Promega) primed with random 9-mers. Quantitative PCR (qPCR) analysis was performed with iTaq Universal SYBR green supermix (Bio-Rad) using the primers listed in Table 1. qPCR was performed on at least three biological replicates and threshold cycle (C_T) values were measured from three technical replicates per biological sample. Fold change was calculated by the $\Delta\Delta C_T$ method.

Affinity purification and Western blotting. To prepare whole-cell lysates for evaluating protein expression of viral ORFs 24 h after transfection, cells were washed with cold DPBS (Gibco) followed by lysis with radioimmunoprecipitation assay (RIPA) lysis buffer (50 mM Tris HCl, 150 mM NaCl, 1.0% [vol/vol] NP-40, 0.5% [wt/vol] sodium deoxycholate, 1.0 mM EDTA, and 0.1% [wt/vol] SDS, Roche cOmplete Mini EDTA-free protease inhibitor cocktail). Cell lysates were vortexed briefly, rotated at 4°C for 15 min, and then clarified by centrifugation at $21,000 \times g$ in a tabletop centrifuge at 4°C for 10 min to remove debris. Cell lysates for affinity purification were prepared at 24 h after transfection by washing and pelleting cells in cold DPBS, followed by resuspension in lysis buffer (50 mM Tris HCl, 150 mM NaCl, 0.5% [vol/vol] NP-40, 1.0 mM EDTA, cOmplete, Mini, EDTA-free Protease Inhibitor Cocktail − Roche) and rotation at 4°C for 30 min. Lysates were clarified by centrifugation at $21,000 \times g$ at 4°C for 10 min, and then 1 mg of lysate was incubated with prewashed MagStrep "type 3" XT magnetic beads (IBA LifeSciences) overnight in IP buffer (150 mM NaCl, 50 mM Tris-HCl, pH 7.4). The beads were washed 3 times for 5 min each with IP wash buffer (150 mM NaCl, 50 mM Tris-HCl, pH 7.4, 0.05% NP-40) and eluted with 2× Laemmli sample buffer (Bio-Rad). Then, 30 μg of whole-cell lysate or IP elutions were resolved on 4% to 15% mini-PROTEAN TGX gels (Bio-Rad). Transfers to polyvinylidene difluoride (PVDF) membranes (Bio-Rad) were done with the Trans-Blot Turbo transfer system (Bio-Rad). Blots were incubated in 5% milk in TBS with 0.1% Tween 20 (TBS-T) to block, followed by incubation with primary antibodies against Strep Tag II antibody horseradish peroxidase (HRP) conjugate (Sigma, 1:5,000), anti-FLAG antibody (Sigma F7425, 1:2,500), anti-GAPDH monoclonal antibody (Invitrogen AM4300, 1:5,000), anti-Vinculin antibody (abcam ab91459, 1;5,000), rabbit polyclonal antiserum to ORF45 (generously provided by Ren Sun [54]), anti-phospho-p44/42 MAPK (Erk1/2) (Thr202/Tyr204) antibody (Cell Signaling no. 9101, 1:1,000), anti-p44/42 MAPK (ERK1/2) antibody (Cell Signaling no. 4695P, 1:1,000), anti-Brf1polyclonal antibody (Bethyl, 1:1,000), or anti Ha-Ras antibody (Sigma MC57, 1:1,000) in 5% milk in TBS-T. Washes were carried out with TBS-T. Blots

were then incubated with HRP-conjugated secondary antibodies (Southern Biotechnology, 1:5,000). Washed blots were incubated with Clarity Western ECL substrate (Bio-Rad) for 5 min and visualized with a ChemiDoc imager (Bio-Rad).

Immunofluorescence. At 24 h posttransfection, NIH 3T3 fibroblasts were plated on coverslips (7.5 × 10^4 cells/well of a 12-well plate) and then fixed in 4% formaldehyde for 10 min. Cells were permeabilized with ice-cold methanol at −20°C for 20 min and incubated with rabbit polyclonal antiserum to ORF45 (generously provided by Ren Sun [54]; 1:200) in 5% BSA overnight at 4°C. Then Alexa Flour 488 goat anti-rabbit IgG antibody (Invitrogen) was added (1:1,000) for 1 h at room temperature. Coverslips were mounted in 4′,6-diamidino-2-phenylindole (DAPI)-containing Vectashield (VectorLabs). Imaging was performed using a confocal Zeiss LSM 880 NLO AxioExaminer microscope driven by Zen 2 software with a 40× water immersion objective (Zeiss and 1.0 NA). Image analysis was performed in FIJI, including image cropping, and brightness/contrast adjustments (103).

SUPPLEMENTAL MATERIAL

Supplemental material is available online only.
SUPPLEMENTAL FILE 1, PDF file, 0.2 MB.

REFERENCES

1. Lander ES, Linton LM, Birren B, Nusbaum C, Zody MC, Baldwin J, Devon K, Dewar K, Doyle M, FitzHugh W, Funke R, Gage D, Harris K, Heaford A, Howland J, Kann L, Lehoczky J, LeVine R, McEwan P, McKernan K, Meldrim J, Mesirov JP, Miranda C, Morris W, Naylor J, Raymond C, Rosetti M, Santos R, Sheridan A, Sougnez C, Stange-Thomann N, Stojanovic N, Subramanian A, Wyman D, Rogers J, Sulston J, Ainscough R, Beck S, Bentley D, Burton J, Clee C, Carter N, Coulson A, Deadman R, Deloukas P, Dunham A, Dunham I, Durbin R, French L, Grafham D, International Human Genome Sequencing Consortium, et al. 2001. Initial sequencing and analysis of the human genome. Nature 409:860–921. https://doi.org/10.1038/35057062.
2. Cordaux R, Batzer MA. 2009. The impact of retrotransposons on human genome evolution. Nat Rev Genet 10:691–703. https://doi.org/10.1038/nrg2640.
3. Kramerov DA, Vassetzky NS. 2011. Origin and evolution of SINEs in eukaryotic genomes. Heredity (Edinb) 107:487–495. https://doi.org/10.1038/hdy.2011.43.
4. Kramerov DA, Vassetzky NS. 2011. SINEs. Wiley Interdiscip Rev RNA 2:772–786. https://doi.org/10.1002/wrna.91.
5. Weiner AM. 1980. An abundant cytoplasmic 7S RNA is complementary to the dominant interspersed middle repetitive DNA sequence family in the human genome. Cell 22:209–218. https://doi.org/10.1016/0092-8674(80)90169-5.
6. Kriegs JO, Churakov G, Jurka J, Brosius J, Schmitz J. 2007. Evolutionary history of 7SL RNA-derived SINEs in supraprimates. Trends Genet 23:158–161. https://doi.org/10.1016/j.tig.2007.02.002.
7. Ullu E, Tschudi C. 1984. Alu sequences are processed 7SL RNA genes. Nature 312:171–172. https://doi.org/10.1038/312171a0.
8. Daniels GR, Deininger PL. 1985. Repeat sequence families derived from mammalian tRNA genes. Nature 317:819–822. https://doi.org/10.1038/317819a0.
9. Tsirigos A, Rigoutsos I. 2009. Alu and B1 repeats have been selectively retained in the upstream and intronic regions of genes of specific functional classes. PLoS Comput Biol 5:e1000610. https://doi.org/10.1371/journal.pcbi.1000610.
10. Chen C, Gentles AJ, Jurka J, Karlin S. 2002. Genes, pseudogenes, and Alu sequence organization across human chromosomes 21 and 22. Proc Natl Acad Sci U S A 99:2930.
11. Korenberg JR, Rykowski MC. 1988. Human genome organization: Alu, LINES, and the molecular structure of metaphase chromosome bands. Cell 53:391–400. https://doi.org/10.1016/0092-8674(88)90159-6.

12. Ferrigno O, Virolle T, Djabari Z, Ortonne J-P, White RJ, Aberdam D. 2001. Transposable B2 SINE elements can provide mobile RNA polymerase II promoters. Nat Genet 28:77–81. https://doi.org/10.1038/ng0501-77.
13. Elbarbary RA, Lucas BA, Maquat LE. 2016. Retrotransposons as regulators of gene expression. Science 351:aac7247. https://doi.org/10.1126/science.aac7247.
14. Su M, Han D, Boyd-Kirkup J, Yu X, Han J-Dong J. 2014. Evolution of alu elements toward enhancers. Cell Rep 7:376–385. https://doi.org/10.1016/j.celrep.2014.03.011.
15. Bourque G, Leong B, Vega VB, Chen X, Lee YL, Srinivasan KG, Chew J-L, Ruan Y, Wei C-L, Ng HH, Liu ET. 2008. Evolution of the mammalian transcription factor binding repertoire via transposable elements. Genome Res 18:1752–1762. https://doi.org/10.1101/gr.080663.108.
16. Laperriere D, Wang T-T, White JH, Mader S. 2007. Widespread Alu repeat-driven expansion of consensus DR2 retinoic acid response elements during primate evolution. BMC Genomics 8:23. https://doi.org/10.1186/1471-2164-8-23.
17. Polak P, Domany E. 2006. Alu elements contain many binding sites for transcription factors and may play a role in regulation of developmental processes. BMC Genomics 7:133. https://doi.org/10.1186/1471-2164-7-133.
18. Schmidt D, Schwalie PC, Wilson MD, Ballester B, Gonçalves Â, Kutter C, Brown GD, Marshall A, Flicek P, Odom DT. 2012. Waves of retrotransposon expansion remodel genome organization and CTCF binding in multiple mammalian lineages. Cell 148:335–348. https://doi.org/10.1016/j.cell.2011.11.058.
19. Sundaram V, Cheng Y, Ma Z, Li D, Xing X, Edge P, Snyder MP, Wang T. 2014. Widespread contribution of transposable elements to the innovation of gene regulatory networks. Genome Res 24:1963–1976. https://doi.org/10.1101/gr.168872.113.
20. Roman AC, Benitez DA, Carvajal-Gonzalez JM, Fernandez-Salguero PM. 2008. Genome-wide B1 retrotransposon binds the transcription factors dioxin receptor and Slug and regulates gene expression in vivo. Proc Natl Acad Sci U S A 105:1632–1637.
21. Román AC, González-Rico FJ, Moltó E, Hernando H, Neto A, Vicente-Garcia C, Ballestar E, Gómez-Skarmeta JL, Vavrova-Anderson J, White RJ, Montoliu L, Fernández-Salguero PM. 2011. Dioxin receptor and SLUG transcription factors regulate the insulator activity of B1 SINE retrotransposons via an RNA polymerase switch. Genome Res 21:422–432. https://doi.org/10.1101/gr.111203.110.

22. Roy-Engel AM, El-Sawy M, Farooq L, Odom GL, Perepelitsa-Belancio V, Bruch H, Oyeniran OO, Deininger PL. 2005. Human retroelements may introduce intragenic polyadenylation signals. Cytogenet Genome Res 110:365–371. https://doi.org/10.1159/000084968.

23. Chen C, Ara T, Gautheret D. 2009. Using Alu elements as polyadenylation sites: a case of retroposon exaptation. Mol Biol Evol 26:327–334. https://doi.org/10.1093/molbev/msn249.

24. Chen L-L, DeCerbo JN, Carmichael GG. 2008. Alu element-mediated gene silencing. EMBO J 27:1694–1705. https://doi.org/10.1038/emboj.2008.94.

25. Gong C, Maquat LE. 2011. lncRNAs transactivate STAU1-mediated mRNA decay by duplexing with 3' UTRs via Alu elements. Nature 470:284–288. https://doi.org/10.1038/nature09701.

26. Gong C, Tang Y, Maquat LE. 2013. mRNA–mRNA duplexes that autoelicit Staufen1-mediated mRNA decay. Nat Struct Mol Biol 20:1214–1220. https://doi.org/10.1038/nsmb.2664.

27. Wang J, Gong C, Maquat LE. 2013. Control of myogenesis by rodent SINE-containing lncRNAs. Genes Dev 27:793–804. https://doi.org/10.1101/gad.212639.112.

28. Varshney D, Vavrova-Anderson J, Oler AJ, Cowling VH, Cairns BR, White RJ. 2015. SINE transcription by RNA polymerase III is suppressed by histone methylation but not by DNA methylation. Nat Commun 6:6569. https://doi.org/10.1038/ncomms7569.

29. Liu W-M, Maraia RJ, Rubin CM, Schmid CW. 1994. Alu transcripts: cytoplasmic localization and regulation by DNA methylation. Nucleic Acids Res 22:1087–1095. https://doi.org/10.1093/nar/22.6.1087.

30. Kondo Y, Issa J-PJ. 2003. Enrichment for histone H3 lysine 9 methylation at alu repeats in human cells*. J Biol Chem 278:27658–27662. https://doi.org/10.1074/jbc.M304072200.

31. Ichiyanagi K, Li Y, Watanabe T, Ichiyanagi T, Fukuda K, Kitayama J, Yamamoto Y, Kuramochi-Miyagawa S, Nakano T, Yabuta Y, Seki Y, Saitou M, Sasaki H. 2011. Locus- and domain-dependent control of DNA methylation at mouse B1 retrotransposons during male germ cell development. Genome Res 21:2058–2066. https://doi.org/10.1101/gr.123679.111.

32. Englander EW, Wolffe AP, Howard BH. 1993. Nucleosome interactions with a human Alu element. Transcriptional repression and effects of template methylation. J Biol Chem 268:19565–19573.

33. Fornace AJ, Jr, Mitchell JB. 1986. Induction of B2 RNA polymerase III transcription by heat shock: enrichment for heat shock induced sequences in rodent cells by hybridization subtraction. Nucleic Acids Res 14:5793–5811. https://doi.org/10.1093/nar/14.14.5793.

34. Jang KL, Latchman DS. 1989. HSV infection induces increased transcription of Alu repeated sequences by RNA polymerase III. FEBS Lett 258:255–258. https://doi.org/10.1016/0014-5793(89)81667-9.

35. Liu W-M, Chu W-M, Choudary PV, Schmid CW. 1995. Cell stress and translational inhibitors transiently increase the abundance of mammalian SINE transcripts. Nucleic Acids Res 23:1758–1765. https://doi.org/10.1093/nar/23.10.1758.

36. Panning B, Smiley JR. 1993. Activation of RNA polymerase III transcription of human Alu repetitive elements by adenovirus type 5: requirement for the E1b 58-kilodalton protein and the products of E4 open reading frames 3 and 6. Mol Cell Biol 13:3231–3244. https://doi.org/10.1128/mcb.13.6.3231-3244.1993.

37. Panning B, Smiley JR. 1994. Activation of RNA polymerase III transcription of human Alu elements by herpes simplex virus. Virology 202:408–417. https://doi.org/10.1006/viro.1994.1357.

38. Williams WP, Tamburic L, Astell CR. 2004. Increased levels of B1 and B2 SINE transcripts in mouse fibroblast cells due to minute virus of mice infection. Virology 327:233–241. https://doi.org/10.1016/j.virol.2004.06.040.

39. Karijolich J, Abernathy E, Glaunsinger BA. 2015. Infection-induced retrotransposon-derived noncoding RNAs enhance herpesviral gene expression via the NF-κB pathway. PLoS Pathog 11:e1005260. https://doi.org/10.1371/journal.ppat.1005260.

40. Singh K, Carey M, Saragosti S, Botchan M. 1985. Expression of enhanced levels of small RNA polymerase III transcripts encoded by the B2 repeats in simian virus 40-transformed mouse cells. Nature 314:553–556. https://doi.org/10.1038/314553a0.

41. Felton-Edkins ZA, Kondrashov A, Karali D, Fairley JA, Dawson CW, Arrand JR, Young LS, White RJ. 2006. Epstein-Barr virus induces cellular transcription factors to allow active expression of EBER genes by RNA polymerase III*. J Biol Chem 281:33871–33880. https://doi.org/10.1074/jbc.M600468200.

42. Diebel KW, Claypool DJ, van Dyk LF. 2014. A conserved RNA polymerase III promoter required for gammaherpesvirus TMER transcription and microRNA processing. Gene 544:8–18. https://doi.org/10.1016/j.gene.2014.04.026.

43. Hoeffler WK, Roeder RG. 1985. Enhancement of RNA polymerase III transcription by the E1A gene product of adenovirus. Cell 41:955–963. https://doi.org/10.1016/s0092-8674(85)80076-3.

44. Tucker JM, Schaller AM, Willis I, Glaunsinger BA, Horner SM. 2020. Alteration of the premature tRNA landscape by gammaherpesvirus infection. mBio 11:e02664-20. https://doi.org/10.1128/mBio.02664-20.

45. Dremel SE, Sivrich FL, Tucker JM, Glaunsinger BA, DeLuca NA. 2022. Manipulation of RNA polymerase III by herpes simplex virus-1. Nat Commun 13:623. https://doi.org/10.1038/s41467-022-28144-8.

46. Allen TA, Von Kaenel S, Goodrich JA, Kugel JF. 2004. The SINE-encoded mouse B2 RNA represses mRNA transcription in response to heat shock. Nat Struct Mol Biol 11:816–821. https://doi.org/10.1038/nsmb813.

47. Mariner PD, Walters RD, Espinoza CA, Drullinger LF, Wagner SD, Kugel JF, Goodrich JA. 2008. Human Alu RNA is a modular transacting repressor of mRNA transcription during heat shock. mol Cell 29:499–509. https://doi.org/10.1016/j.molcel.2007.12.013.

48. Yakovchuk P, Goodrich JA, Kugel JF. 2009. B2 RNA and Alu RNA repress transcription by disrupting contacts between RNA polymerase II and promoter DNA within assembled complexes. Proc Natl Acad Sci U S A 106:5569–5574. https://doi.org/10.1073/pnas.0810738106.

49. Di Ruocco F, Basso V, Rivoire M, Mehlen P, Ambati J, De Falco S, Tarallo V. 2018. Alu RNA accumulation induces epithelial-to-mesenchymal transition by modulating miR-566 and is associated with cancer progression. Oncogene 37:627–637. https://doi.org/10.1038/onc.2017.369.

50. Kaneko H, Dridi S, Tarallo V, Gelfand BD, Fowler BJ, Cho WG, Kleinman ME, Ponicsan SL, Hauswirth WW, Chiodo VA, Karikó K, Yoo JW, Lee D-k, Hadziahmetovic M, Song Y, Misra S, Chaudhuri G, Buaas FW, Braun RE, Hinton DR, Zhang Q, Grossniklaus HE, Provis JM, Madigan MC, Milam AH, Justice NL, Albuquerque RJC, Blandford AD, Bogdanovich S, Hirano Y, Witta J, Fuchs E, Littman DR, Ambati BK, Rudin CM, Chong MMW, Provost P, Kugel JF, Goodrich JA, Dunaief JL, Baffi JZ, Ambati J. 2011. DICER1 deficit induces Alu RNA toxicity in age-related macular degeneration. Nature 471:325–330. https://doi.org/10.1038/nature09830.

51. Tarallo V, Hirano Y, Gelfand BD, Dridi S, Kerur N, Kim Y, Cho WG, Kaneko H, Fowler BJ, Bogdanovich S, Albuquerque RJ, Hauswirth WW, Chiodo VA, Kugel JF, Goodrich JA, Ponicsan SL, Chaudhuri G, Murphy MP, Dunaief JL, Ambati BK, Ogura Y, Yoo JW, Lee D-k, Provost P, Hinton DR, Núñez G, Baffi JZ, Kleinman ME, Ambati J. 2012. DICER1 Loss and Alu RNA induce age-related macular degeneration via the NLRP3 inflammasome and MyD88. Cell 149:847–859. https://doi.org/10.1016/j.cell.2012.03.036.

52. Karijolich J, Zhao Y, Alla R, Glaunsinger B. 2017. Genome-wide mapping of infection-induced SINE RNAs reveals a role in selective mRNA export. Nucleic Acids Res 45:6194–6208. https://doi.org/10.1093/nar/gkx180.

53. Schaller AM, Tucker J, Willis I, Glaunsinger BA, Sandri-Goldin RM. 2020. Conserved herpesvirus kinase ORF36 activates B2 retrotransposons during murine gammaherpesvirus infection. J Virol 94:e00262-20. https://doi.org/10.1128/JVI.00262-20.

54. Jia Q, Chernishof V, Bortz E, McHardy I, Wu T-T, Liao H-I, Sun R. 2005. Murine gammaherpesvirus 68 open reading frame 45 plays an essential role during the immediate-early phase of viral replication. J Virol 79:5129–5141. https://doi.org/10.1128/JVI.79.8.5129-5141.2005.

55. Avey D, Tepper S, Pifer B, Bahga A, Williams H, Gillen J, Li W, Ogden S, Zhu F, Sandri-Goldin RM. 2016. Discovery of a coregulatory interaction between Kaposi's sarcoma-associated herpesvirus ORF45 and the viral protein kinase ORF36. J Virol 90:5953–5964. https://doi.org/10.1128/JVI.00516-16.

56. Li X, Zhu F. 2009. Identification of the nuclear export and adjacent nuclear localization signals for ORF45 of Kaposi's sarcoma-associated herpesvirus. J Virol 83:2531–2539. https://doi.org/10.1128/JVI.02209-08.

57. Li X, Huang L, Xiao Y, Yao X, Long X, Zhu F, Kuang E, Jung JU. 2019. Development of an ORF45-derived peptide to inhibit the sustained RSK activation and lytic replication of Kaposi's sarcoma-associated herpesvirus. J Virol 93:e02154-18. https://doi.org/10.1128/JVI.02154-18.

58. Kuang E, Tang Q, Maul GG, Zhu F. 2008. Activation of p90 ribosomal s6 kinase by ORF45 of Kaposi's sarcoma-associated herpesvirus and its role in viral lytic replication. J Virol 82:1838–1850. https://doi.org/10.1128/JVI.02119-07.

59. Zhu F, Kuang E, Wu F. 2009. Activation of RSK and ERK MAPK kinases by ORF45 of Kaposi's sarcoma-associated herpesvirus. Infectious Agents and Cancer 4:P48. https://doi.org/10.1186/1750-9378-4-S2-P48.

60. Avey D, Tepper S, Li W, Turpin Z, Zhu F. 2015. Phosphoproteomic analysis of KSHV-infected cells reveals roles of ORF45-activated RSK during lytic replication. PLoS Pathog 11:e1004993. https://doi.org/10.1371/journal.ppat.1004993.

61. Kuang E, Wu F, Zhu F. 2009. Mechanism of Sustained Activation of Ribosomal S6 Kinase (RSK) and ERK by Kaposi Sarcoma-associated Herpesvirus ORF45: multiprotein complexes retain active phosphorylated ERK and RSK and protect them from dephosphorylation*. J Biol Chem 284: 13958–13968. https://doi.org/10.1074/jbc.M900025200.

62. Kuang E, Fu B, Liang Q, Myoung J, Zhu F. 2011. Phosphorylation of eukaryotic translation initiation factor 4B (EIF4B) by open reading frame 45/p90 ribosomal S6 kinase (ORF45/RSK) signaling axis facilitates protein translation during kaposi sarcoma-associated herpesvirus (KSHV) Lytic Replication*. J Biol Chem 286:41171–41182. https://doi.org/10.1074/jbc.M111.280982.

63. Alexa A, Sok P, Gross F, Albert K, Kobori E, Póti ÁL, Gógl G, Bento I, Kuang E, Taylor SS, Zhu F, Ciliberto A, Reményi A. 2022. A non-catalytic herpesviral protein reconfigures ERK-RSK signaling by targeting kinase docking systems in the host. Nat Commun 13:472. https://doi.org/10.1038/s41467-022-28109-x.

64. Stahl JA, Chavan SS, Sifford JM, MacLeod V, Voth DE, Edmondson RD, Forrest JC. 2013. Phosphoproteomic analyses reveal signaling pathways that facilitate lytic gammaherpesvirus replication. PLoS Pathog 9:e1003583. https://doi.org/10.1371/journal.ppat.1003583.

65. Fu B, Kuang E, Li W, Avey D, Li X, Turpin Z, Valdes A, Brulois K, Myoung J, Zhu F, Frueh K. 2015. Activation of p90 ribosomal S6 kinases by ORF45 of Kaposi's sarcoma-associated herpesvirus is critical for optimal production of infectious viruses. J Virol 89:195–207. https://doi.org/10.1128/JVI.01937-14.

66. Favata MF, Horiuchi KY, Manos EJ, Daulerio AJ, Stradley DA, Feeser WS, Van Dyk DE, Pitts WJ, Earl RA, Hobbs F, Copeland RA, Magolda RL, Scherle PA, Trzaskos JM. 1998. Identification of a novel inhibitor of mitogen-activated protein kinase kinase. J Biol Chem 273:18623–18632. https://doi.org/10.1074/jbc.273.29.18623.

67. Goodfellow SJ, Innes F, Derblay LE, MacLellan WR, Scott PH, White RJ. 2006. Regulation of RNA polymerase III transcription during hypertrophic growth. EMBO J 25:1522–1533. https://doi.org/10.1038/sj.emboj.7601040.

68. Goodfellow SJ, White RJ. 2007. Regulation of RNA Polymerase III Transcription During Mammalian Cell Growth. Cell Cycle 6:2323–2326. https://doi.org/10.4161/cc.6.19.4767.

69. Felton-Edkins ZA, Fairley JA, Graham EL, Johnston IM, White RJ, Scott PH. 2003. The mitogen-activated protein (MAP) kinase ERK induces tRNA synthesis by phosphorylating TFIIIB. EMBO J 22:2422–2432. https://doi.org/10.1093/emboj/cdg240.

70. Gomez-Roman N, Grandori C, Eisenman RN, White RJ. 2003. Direct activation of RNA polymerase III transcription by c-Myc. Nature 421:290–294. https://doi.org/10.1038/nature01327.

71. Yeh HH, Wu CH, Giri R, Kato K, Kohno K, Izumi H, Chou CY, Su WC, Liu HS. 2008. Oncogenic Ras-induced morphologic change is through MEK/ERK signaling pathway to downregulate Stat3 at a posttranslational level in NIH3T3 cells. Neoplasia 10:52–60. https://doi.org/10.1593/neo.07691.

72. Colao I, Pennisi R, Venuti A, Nygårdas M, Heikkilä O, Hukkanen V, Sciortino MT. 2017. The ERK-1 function is required for HSV-1-mediated G1/S progression in HEP-2 cells and contributes to virus growth. Sci Rep 7:9176. https://doi.org/10.1038/s41598-017-09529-y.

73. Gaynor RB, Feldman LT, Berk AJ. 1985. Transcription of class III genes activated by viral immediate early proteins. Science 230:447–450. https://doi.org/10.1126/science.2996135.

74. Felton-Edkins ZA, White RJ. 2002. Multiple mechanisms contribute to the activation of RNA polymerase III transcription in cells transformed by papovaviruses*. J Biol Chem 277:48182–48191. https://doi.org/10.1074/jbc.M201333200.

75. van Weringh A, Ragonnet-Cronin M, Pranckeviciene E, Pavon-Eternod M, Kleiman L, Xia X. 2011. HIV-1 modulates the tRNA pool to improve translation efficiency. Mol Biol Evol 28:1827–1834. https://doi.org/10.1093/molbev/msr005.

76. Virgin HW, Latreille P, Wamsley P, Hallsworth K, Weck KE, Canto AJD, Speck SH. 1997. Complete sequence and genomic analysis of murine gammaherpesvirus 68. J Virol 71:5894–5904. https://doi.org/10.1128/JVI.71.8.5894-5904.1997.

77. Jia X, Shen S, Lv Y, Zhang Z, Guo H, Deng H, Longnecker RM. 2016. Tegument protein ORF45 plays an essential role in virion morphogenesis of murine gammaherpesvirus 68. J Virol 90:7587–7592. https://doi.org/10.1128/JVI.03231-15.

78. Song MJ, Hwang S, Wong WH, Wu T-T, Lee S, Liao H-I, Sun R. 2005. Identification of viral genes essential for replication of murine gamma-herpesvirus 68 using signature-tagged mutagenesis. Proc Natl Acad Sci U S A 102: 3805–3810. https://doi.org/10.1073/pnas.0404521102.

79. Ebrahimi B, Dutia BM, Roberts KL, Garcia-Ramirez JJ, Dickinson P, Stewart JP, Ghazal P, Roy DJ, Nash AA. 2003. Transcriptome profile of murine gammaherpesvirus-68 lytic infection. J Gen Virol 84:99–109. https://doi.org/10.1099/vir.0.18639-0.

80. Martinez-Guzman D, Rickabaugh T, Wu T-T, Brown H, Cole S, Song MJ, Tong L, Sun R. 2003. Transcription program of murine gammaherpesvirus 68. J Virol 77:10488–10503. https://doi.org/10.1128/jvi.77.19.10488-10503.2003.

81. Zhu FX, King SM, Smith EJ, Levy DE, Yuan Y. 2002. A Kaposi's sarcoma-associated herpesviral protein inhibits virus-mediated induction of type I interferon by blocking IRF-7 phosphorylation and nuclear accumulation. Proc Natl Acad Sci U S A 99:5573–5578. https://doi.org/10.1073/pnas.082420599.

82. Liang Q, Fu B, Wu F, Li X, Yuan Y, Zhu F. 2012. ORF45 of Kaposi's sarcoma-associated herpesvirus inhibits phosphorylation of interferon regulatory factor 7 by IKKε; and TBK1 as an alternative substrate. J Virol 86: 10162–10172. https://doi.org/10.1128/JVI.05224-11.

83. Zhu FX, Sathish N, Yuan Y. 2010. Antagonism of host antiviral responses by Kaposi's sarcoma-associated herpesvirus tegument protein ORF45. PLoS One 5:e10573. https://doi.org/10.1371/journal.pone.0010573.

84. Johnson LF, Levis R, Abelson HT, Green H, Penman S. 1976. Changes in RNA in relation to growth of the fibroblast. IV. Alterations in theproduction and processing of mRNA and rRNA in resting and growing cells. J Cell Biol 71:933–938. https://doi.org/10.1083/jcb.71.3.933.

85. Mauck JC, Green H. 1974. Regulation of pre-transfer RNA synthesis during transition from resting to growing state. Cell 3:171–177. https://doi.org/10.1016/0092-8674(74)90122-6.

86. Scott PH, Cairns CA, Sutcliffe JE, Alzuherri HM, McLees A, Winter AG, White RJ. 2001. Regulation of RNA polymerase III transcription during cell cycle entry. J Biol Chem 276:1005–1014. https://doi.org/10.1074/jbc.M005417200.

87. Innes F, Ramsbottom B, White RJ. 2006. A test of the model that RNA polymerase III transcription is regulated by selective induction of the 110 kDa subunit of TFIIIC. Nucleic Acids Res 34:3399–3407. https://doi.org/10.1093/nar/gkl432.

88. Sethy-Coraci I, Moir RD, López-de-León A, Willis IM. 1998. A differential response of wild type and mutant promoters to TFIIIB70 overexpression in vivo and in vitro. Nucleic Acids Res 26:2344–2352. https://doi.org/10.1093/nar/26.10.2344.

89. Pleschka S. 2008. RNA viruses and the mitogenic Raf/MEK/ERK signal transduction cascade. Biol Chem 389:1273–1282. https://doi.org/10.1515/BC.2008.145.

90. Panteva M, Korkaya H, Jameel S. 2003. Hepatitis viruses and the MAPK pathway: is this a survival strategy? Virus Res 92:131–140. https://doi.org/10.1016/S0168-1702(02)00356-8.

91. Bonjardim CA. 2017. Viral exploitation of the MEK/ERK pathway – a tale of vaccinia virus and other viruses. Virology 507:267–275. https://doi.org/10.1016/j.virol.2016.12.011.

92. DuShane JK, Maginnis MS. 2019. Human DNA Virus exploitation of the MAPK-ERK cascade. Int J Molecular Sciences 20:3427. https://doi.org/10.3390/ijms20143427.

93. Cohen A, Brodie C, Sarid R. 2006. An essential role of ERK signalling in TPA-induced reactivation of Kaposi's sarcoma-associated herpesvirus. J Gen Virol 87:795–802. https://doi.org/10.1099/vir.0.81619-0.

94. Xie J, Ajibade AO, Ye F, Kuhne K, Gao SJ. 2008. Reactivation of Kaposi's sarcoma-associated herpesvirus from latency requires MEK/ERK, JNK and p38 multiple mitogen-activated protein kinase pathways. Virology 371: 139–154. https://doi.org/10.1016/j.virol.2007.09.040.

95. Yu F, Harada JN, Brown HJ, Deng H, Song MJ, Wu TT, Kato-Stankiewicz J, NeIson CG, Vieira J, Tamanoi F, Chanda SK, Sun R. 2007. Systematic identification of cellular signals reactivating Kaposi sarcoma-associated herpesvirus. PLoS Pathog 3:e44. https://doi.org/10.1371/journal.ppat.0030044.

96. Ford PW, Bryan BA, Dyson OF, Weidner DA, Chintalgattu V, Akula SM. 2006. Raf/MEK/ERK signalling triggers reactivation of Kaposi's sarcoma-associated herpesvirus latency. J Gen Virol 87:1139–1144. https://doi.org/10.1099/vir.0.81628-0.

97. Sarid R, Wiezorek JS, Moore PS, Chang Y. 1999. Characterization and cell cycle regulation of the major Kaposi's sarcoma-associated herpesvirus (human herpesvirus 8) latent genes and their promoter. J Virol 73:1438–1446. https://doi.org/10.1128/JVI.73.2.1438-1446.1999.

98. Akula SM, Ford PW, Whitman AG, Hamden KE, Shelton JG, McCubrey JA. 2004. Raf promotes human herpesvirus-8 (HHV-8/KSHV) infection. Oncogene 23:5227–5241. https://doi.org/10.1038/sj.onc.1207643.

99. Pan H, Xie J, Ye F, Gao S-J. 2006. Modulation of Kaposi's sarcoma-associated herpesvirus infection and replication by MEK/ERK, JNK, and p38 multiple mitogen-activated protein kinase pathways during primary infection. J Virol 80:5371–5382. https://doi.org/10.1128/JVI.02299-05.

100. Naranatt PP, Akula SM, Zien CA, Krishnan HH, Chandran B. 2003. Kaposi's Sarcoma-associated herpesvirus induces the phosphatidylinositol 3-kinase-PKC-zeta-MEK-ERK signaling pathway in target cells early during infection: implications for Infectivity. J Virol 77:1524–1539. https://doi.org/10.1128/jvi.77.2.1524-1539.2003.

101. Sharma-Walia N, Krishnan HH, Naranatt PP, Zeng L, Smith MS, Chandran B. 2005. ERK1/2 and MEK1/2 induced by Kaposi's sarcoma-associated herpesvirus (human herpesvirus 8) early during infection of target cells are essential for expression of viral genes and for establishment of infection. J Virol 79:10308–10329. https://doi.org/10.1128/JVI.79.16.10308-10329.2005.

102. Sedlackova L, Rice SA. 2008. Herpes simplex virus type 1 immediate-early protein ICP27 Is required for efficient incorporation of ICP0 and ICP4 into virions. J Virol 82:268–277. https://doi.org/10.1128/JVI.01588-07.

103. Schindelin J, Arganda-Carreras I, Frise E, Kaynig V, Longair M, Pietzsch T, Preibisch S, Rueden C, Saalfeld S, Schmid B, Tinevez J-Y, White DJ, Hartenstein V, Eliceiri K, Tomancak P, Cardona A. 2012. Fiji: an open-source platform for biological-image analysis. Nat Methods 9:676–682. https://doi.org/10.1038/nmeth.2019.